European Radiology (2019) 29:1820–1830
https://doi.org/10.1007/s00330-018-5751-1

UROGENITAL

Histopathological to multiparametric MRI spatial mapping of extended systematic sextant and MR/TRUS-fusion-targeted biopsy of the prostate

David Bonekamp[1] · Patrick Schelb[1] · Manuel Wiesenfarth[2] · Tristan Anselm Kuder[3] · Fenja Deister[3] · Albrecht Stenzinger[4] · Joanne Nyarangi-Dix[5] · Matthias Röthke[1] · Markus Hohenfellner[5] · Heinz-Peter Schlemmer[1] · Jan Philipp Radtke[1,5]

Received: 19 May 2018 / Revised: 15 August 2018 / Accepted: 11 September 2018 / Published online: 16 October 2018

Abstract

Purpose MRI has limited ability to detect multifocal disease or the full extent of prostate involvement with clinically significant prostate cancer (sPC). We compare the spatial co-localization at sextant resolution of MRI lesions and histopathological mapping by combined targeted and extended systematic biopsies.

Materials and methods Sextants were mapped for sPC (ISUP group ≥ 2) by 24-core transperineal systematic biopsies in 316 patients with suspicion for sPC and by MR lesions of PI-RADS score of ≥ 3. The gold standard is combined systematic (median 23 cores) and targeted biopsies.

Results Of 316 men, 121 (38%) harbored sPC. Of these 121 patients, 4 (3%) had a negative MRI. MRI correctly identified 117/121 (97%) patients with sPC. In these patients, mpMRI missed no additional sPC in 96 (82%), while MRI-negative sPC lesions were present in 21 patients (18%). Of 1896 sextants, 379 (20%) harbored sPC. MR-positive sextants contained sPC in 26% (337/1275), compared to 7% (42/621) in MR-negative sextants. On a patient basis, sensitivity was 0.97, specificity 0.22, positive predictive value 0.43, and negative predictive value 0.91. On a sextant basis, sensitivity was 0.73, specificity 0.38, positive predictive value 0.26, and negative predictive value 0.93.

Conclusion MpMRI mapping agreed well with histopathology with, at the observed sPC prevalence and on a patient basis, excellent sensitivity and negative predictive value, and acceptable specificity and positive predictive value for sPC. However, 18% of sPC was outside the mpMRI mapped region, quantifying limitations of MRI for complete localization of disease extent.

Key Points

- *Currently, exclusive MRI mapping of the prostate for focal treatment planning cannot be recommended, as significant prostate cancer may remain untreated in a substantial number of cases.*
- *At the observed sPC prevalence and on a patient basis, mpMRI has excellent sensitivity and NPV, and acceptable specificity and PPV for detection of prostate cancer, supporting its use to detect suspicious lesions before biopsy.*
- *Despite the excellent global performance, 18% of sPC was outside the mpMRI mapped region even when a security margin of 10 mm was considered, indicating that prostate MRI has limited ability to completely map all cancer foci within the prostate.*

Keywords Male · Prostate cancer · Magnetic resonance imaging · Image-guided biopsy

Electronic supplementary material The online version of this article (https://doi.org/10.1007/s00330-018-5751-1) contains supplementary material, which is available to authorized users.

✉ David Bonekamp
d.bonekamp@dkfz-heidelberg.de

[1] Department of Radiology, German Cancer Research Center (DKFZ), Im Neuenheimer Feld 280, 69120 Heidelberg, Germany

[2] Division of Statistics, German Cancer Research Center (DKFZ), Heidelberg, Germany

[3] Department of Medical Physics, German Cancer Research Center (DKFZ), Heidelberg, Germany

[4] Institute of Pathology, University of Heidelberg Medical Center, Heidelberg, Germany

[5] Department of Urology, University of Heidelberg Medical Center, Heidelberg, Germany

Abbreviations

AS	Active surveillance
Bx	Biopsy
DCE	Dynamic contrast-enhanced imaging
DRE	Digital-rectal examination
DWI	Diffusion-weighted imaging
EPI	Echo-planar imaging
GP	Gleason pattern
GS	Gleason score
ISUP	International Society of Urological Pathology
mpMRI	Multiparametric magnetic resonance imaging
MRI	Magnetic resonance imaging
NPV	Negative predictive value
PC	Prostate cancer
PI-RADS	Prostate Imaging Reporting and Data System
PPV	Positive predictive value
PSA	Prostate specific antigen
RP	Radical prostatectomy
SB	Systematic transperineal saturation
sPC	Significant prostate cancer
STARD	Standards of Reporting of Diagnostic Accuracy
START	Standards of Reporting for MRI-targeted Biopsy Studies
TB	MRI-targeted biopsy
TRUS	Transrectal ultrasound

Introduction

The role of multiparametric magnetic resonance imaging (mpMRI) in prostate cancer (PC) management has constantly evolved during the last decade [1, 2]. It is currently recommended to target MR lesions in men suspected of harboring PCa despite negative systematic biopsies, and MRI is increasingly being used to guide biopsies in biopsy-naïve men, due to the high accuracy of MRI-guided targeted biopsy techniques [3–6]. Most recently, the utilization of MRI as a triage test prior to biopsy has been proven by the PROMIS and PRECISION trials [7, 8]. Nonetheless, MRI has limited ability to detect multifocal disease or the full extent of prostate involvement with clinically significant prostate cancer (sPC).

A recent study of Kenigsberg et al reported that Gleason pattern (GP) 4 extra-focal disease defined as any GP 4 not detected by mpMRI and transrectal ultrasound systematic biopsy outside of an ablation zone was present in 15/59 (25%) of cases [9]. Of these, 35% were ipsilateral and 65% contralateral to MRI [9]. 80% were Gleason score (GS) 3 + 4 (International Society of Urological Pathology, (ISUP) Grade 2), 10% GS 4 + 3 (ISUP Grade 3), and 10% GS 4 + 4 (ISUP Grade 4) [9]. Only 50% of these were less than 5 mm in cross-sectional length on radical prostatectomy (RP) specimen [9]. Ablation of only the MRI lesion plus a 10-mm margin or performing an ipsilateral hemi-ablation would have left residual GP 4 tumor foci in 24% and 19% of cases [9]. However, using biopsies as reference tests, the negative predictive value (NPV) to rule out sPC was 88–95% [1, 10]. Recent studies using RP specimen as reference test demonstrated that about 85% of sPC foci were correctly identified by mpMRI using the Prostate Imaging Reporting and Data System (PI-RADS) [11, 12].

The purpose of this study was to compare the spatial accuracy of mpMRI to the combined mapping information of all extended systematic and targeted biopsy cores on MRI/transrectal ultrasound (TRUS)-fusion biopsies. Specifically, we analyzed spatial agreement on sextant, hemisphere, and patient bases.

Material and methods

This retrospective analysis was performed in a patient cohort of a previously reported study [13]. The institutional and governmental ethics committee approved the study and waived informed consent. This study analysis included the patient data of the prior study of which an analysis has been published previously regarding a comparison of radiomic machine learning with ADC values [13]. In comparison, here, we investigate spatial co-localization of MRI-detected lesions to systematic and targeted biopsies that has not been evaluated previously.

Patient cohort

The examined patient cohort includes 316 consecutive patients with a clinical indication for prostate biopsy based on PSA elevation and clinical examination or participation in our active surveillance program who were examined on a single 3T MR System in 2015–2016 and subsequently underwent MRI/TRUS-fusion biopsy at our institution. Inclusion and exclusion criteria have been described previously [13]. Baseline epidemiological and clinical characteristics including tumor location, pathological findings, and clinical assessment are shown in Table 1.

MR imaging

MR images were acquired at 3 Tesla (Magnetom Prisma, Siemens Healthcare, Erlangen, Germany) using the standard multi-channel body coil and integrated spine phased-array coil, according to the European Society of Urogenital Radiology (ESUR) guidelines [2]. As per the institutional protocol, axial, coronal, and sagittal T2-weighted (T2) images, echo-planar imaging (EPI) diffusion-weighted images (DWI), and dynamic contrast-enhanced (DCE) images were acquired. The full diagnostic prostate MRI protocol is shown in Supplementary Table 1. Clinical interpretation by board-

Table 1 Patients' epidemiological and clinical characteristics according to START criteria [14]

Men included in analysis	(*n* = 316)
Age (years)	
Median (IQR)	64 (58–71)
sPC found in MR Lesion (*n* (%))	140 (30%)
peripheral zone	91 (20%)
transition zone	49 (11%)
No sPC found in MR Lesion	322 (70%)
Pre-Biopsy PSA (ng/ml) median (IQR)	6.9 (5.0–9.9)
Pre-Biopsy PSA density median (IQR)	0.16 (0.10–0.24)
Suspicious DRE	91 (29%)
Number of previous biopsy cores (range)	12 (10–14)
MR index lesion per patient (*n* (%))	
No Lesion	38 (12%)
PI-RADS 2	12 (4%)
PI-RADS 3	72 (23%)
PI-RADS 4	114 (36%)
PI-RADS 5	80 (25%)
MRI assessment per lesion (*n* (%))	
Total	462 (100%)
PI-RADS 2	25 (5%)
PI-RADS 3	162 (35%)
PI-RADS 4	179 (39%)
PI-RADS 5	96 (21%)
Patients without MR Lesions	38
Patients with MR Lesions	278 (100%)
Number of MR	
Lesions per patient (*n* (%))	
1 lesion	133 (48%)
2 lesions	111 (40%)
3 lesions	29 (10%)
4 lesions	5 (2%)
Days MRI to biopsy, median (IQR)	1 (1–9)
Number of cores per patient (median, range)	29 (24–33)
Targeted cores per lesion	4 (3–5)
Systematic cores	23 (20–26)
Per-patient MR/TRUS Gleason score/ISUP grade (*n* (%))	
No PC	126 (40%)
6 (3 + 3)/1	69 (22%)
7a (3 + 4)/2	80 (25%)
7b (4 + 3)/3	15 (5%)
8 (4 + 4)/4	12 (4%)
9a (4 + 5)/5	9 (3%)
9b (5 + 4)/5	5 (2%)

IQR interquartile range, *PSA* prostate-specific antigen, *MRI* magnetic resonance imaging, *PI-RADS* Prostate Imaging Reporting and Data System, *sPC* clinically significant PC, *ISUP* International Society of Urologic Pathology, *DRE* digital rectal examination

certified radiologists included PI-RADS assessment for each detected lesion and a pictogram indicating lesion location [15].

Systematic and targeted MRI/TRUS-fusion biopsies

All men underwent transperineal grid-directed biopsy performed under general anesthesia with rigid software registration using BiopSee (MEDCOM, Darmstadt, Germany). Targeted fusion biopsy (FTB) of MRI-suspicious lesions was performed first (interquartile range (IQR) 3–5 cores, median 4 per lesion) followed by systematic saturation biopsy (20–26 cores, median 23 cores), as previously described [4, 12]. This biopsy approach combining FTBs and transperineal systematic saturation biopsies (SBs) has been validated against and confirmed concordance to RP specimen [12]. A median of 29 biopsies (IQR 24–33) were taken per patient with the number of biopsies adjusted to prostate volume [16]. Histopathological results of targeted regions and whole-gland assessment served as standard of reference. Most importantly, according to the Ginsburg Study group protocol, a sextant scheme of the prostate tailored to the transperineal approach has been used for analysis of the correct identification of the lesions' localization [16].

MR lesion segmentation

Apparent diffusion coefficient (ADC), *b* value = 1500 s/mm^2 (B1500), and T2w images were upsampled to 0.25-mm in-plane resolution and 3-mm slice thickness using the medical imaging toolkit (MITK, www.mitk.org) [17, 18]. Three-dimensional (3D) volumes of interest (VOI) were manually drawn using the MITK polygon tool by one investigator (P.S. with 6 months experience in prostate MRI) separately on T2w images and ADC images using series and slice information and pictograms given in the clinical reports under supervision of a board-certified radiologist with 8 years of experience in prostate MRI (D.B.). A total of 462 lesions were segmented. In addition, prostate contours were segmented manually on T2w images and automatically partitioned into sextants using the midsagittal plane and four additional angulated planes according to the biopsy protocol, and named RA, RM, and RP and LA, LM, and LP, indicating right/left and anterior/mid/posterior locations, respectively [16]. Figure 1 depicts example segmentations of lesions and sextants (see figure legends for details).

Pathological workup

Histopathological analyses were performed under supervision of one dedicated uropathologist (A.S., 6-year experience) according to International Society of Urological Pathology standards.

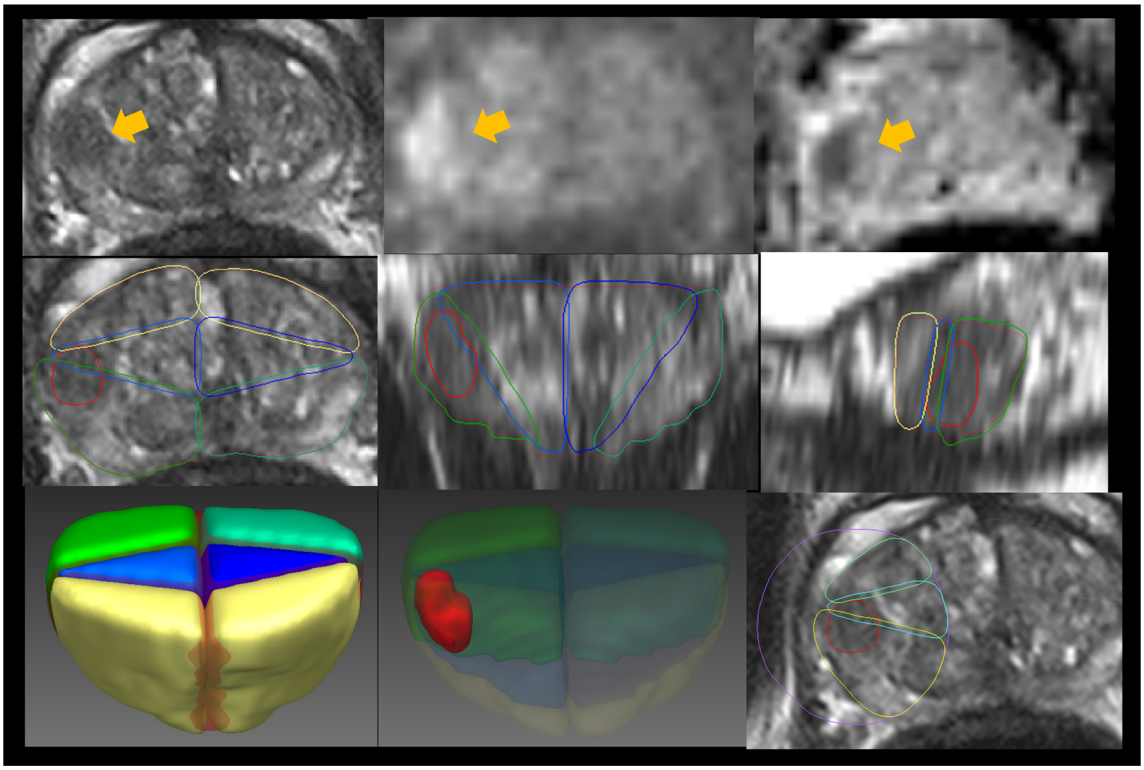

Fig. 1 Figure illustrating post-processing of MR imaging. Top panel: axial T2-weighted image (left), *b* value = 1500 s/mm^2 image (middle) and ADC map (right) demonstrate a suspicious lesion (arrows) in PZa/PZpl in the right midportion of the prostate with marked signal increase on *b* = 1500, a markedly decreased ADC value and suspicious homogeneous hypointensity on the T2w image, PI-RADS 5. Middle panel: sextants are spatially defined as shown for right and left anterior (yellow), middle (blue), and posterior (green) locations and shown together with the radiologically defined lesion (red) in axial (left), coronal (middle), and sagittal (right) planes. Bottom panel: volume renderings of the prostate segmentation seen from anteriorly superiorly with sextants shown (left) and lesion shown by decreasing the opacity of the sextant volumes (middle). The right diagram shows the definition of the zonal safety margin of 10 mm (purple) around the radiological lesion (red), with segmentation and masking of this zonal margin according to sextants and prostate boundary (green, cyan, and yellow contours from anteriorly to posteriorly), defining the three right (RA, RM, RP) of six sextants to be formally considered positive within the security margin

Image post-processing and statistical analysis

Recently, Le Nobin et al published that MRI underestimated the boundaries of PC lesions compared to RPE specimen. They proposed a three-dimensional security margin of 10 mm around the MRI lesion to account for lesion underestimation by MRI [19]. Accordingly, all lesion VOIs were not only analyzed as they appeared, but in addition were automatically dilated to generate a set of VOIs including a security margin of 10 mm around MR lesions [19]. The intersections of standard and dilated VOIs with sextant VOIs were determined and sextants assigned the maximum PI-RADS score given to any intersecting MR lesion. Sextant-specific systematic biopsy histopathology was assigned to all MR sextant VOIs and augmented by calculating the maximum ISUP grade between systematic histopathology and histopathology from FTB to sextants intersecting with MR lesions (the latter was performed only for standard VOIs and not for dilated VOIs) to create a sextant map of histopathology ground truth. SPC was defined as ISUP grade ≥ 2 and a positive MRI as a PI-RADS score of ≥ 3 in any lesion.

Spatial matching between the histopathological ground truth map and mpMRI mapping was performed on standard VOIs and dilated VOIs. In addition to sextant spatial matching based on the Ginsburg scheme, it was determined if hemispheres could be identified that were predicted free of sPC by mpMRI [16]. Sensitivity, specificity, PPV, and NPV were calculated for standard and dilated lesion VOIs on (i) a sextant, ii) a hemisphere basis, and (iii) for the whole prostate, by examining the coincidence of pathological and radiological index lesions at the respective degree of spatial resolution. An additional stratification according to a history of no prior biopsy, prior negative biopsy, and active surveillance was performed to investigate effects on the distribution of sPC. The distribution of sPC across patients, hemispheres, and sextants was calculated and depicted as flow diagrams.

Statistical analyses were performed using R version 3.3.0 (R Foundation for Statistical Computing, Vienna, Austria) [20]. Reporting followed Standards of Reporting of Diagnostic Accuracy (Supplementary Material 2) [21].

Results

Of the 316 patients included in the study, 173 (55%) were biopsy naïve, 94 (30%) had received one to five prior negative biopsies (one: 62, two: 23, three: 4, four: 3 and five: 2 patients, respectively), and 49 (16%) were enrolled into active surveillance at the time of the MR exam.

In total, 121 of 316 patients (38%) harbored at least one sPC lesion. Clinical data and pathological outcome according to the Standards of Reporting for MRI-targeted Biopsy Studies (START) are provided in Table 1. On per-patient analysis (Fig. 2), 269 men were MR positive and 47 men were MR negative. One hundred seventeen out of the 269 MR-positive men harbored sPC while 152 were false positive. For MRI-negative patients, 43 out of 47 were correctly called negative on MRI, while MRI did not detect four sPC-positive men. Sensitivity was 0.97, specificity 0.22, positive predictive value (PPV) 0.43, and negative predictive value (NPV) 0.91. The results for sPC definition as ISUP grade ≥ 3 and MRI suspicion defined as PI-RADS ≥ 4 are shown in Supplementary Figure 2–4.

On the hemisphere level (Fig. 3), 192 of 632 hemispheres (30%) harbored sPC. 396 (63%) hemispheres were MR positive and 236 (37%) were MRI negative. One hundred sixty six (42%) out of the 396 MR-positive hemispheres harbored sPC, while 230 (58%) were false positive. For MRI-negative hemispheres, 210 (89%) of 236 were correctly called negative on MRI, while MRI did not detect sPC presence in 26 (11%) of hemispheres. Sensitivity was 0.86, specificity 0.48, PPV 0.42, and NPV 0.89 (Table 2). Hemispheric results for sPC definition as ISUP grade ≥ 3 and MRI suspicion defined as PI-RADS ≥ 4 are given in Supplementary Figure 6–8.

On the sextant level (Fig. 4), 379 of 1896 sextants (20%) harbored sPC. 660 (35%) sextants were MR positive and 1236 (65%) were MRI negative. Two hundred fifty-four (38%) out of the 660 MR-positive sextants harbored sPC, while 406 (62%) were false positive. For MRI-negative sextants, 1111 (90%) of 1236 were correctly called negative on MRI, while MRI did not detect sPC presence in 125 (10%) of sextants. Sensitivity was 0.67, specificity 0.73, PPV 0.38, and NPV 0.90 (Table 2).

On the sextant level including the security margin of 10 mm, 379 of 1896 sextants (20%) harbored sPC. 1275 (67%) sextants

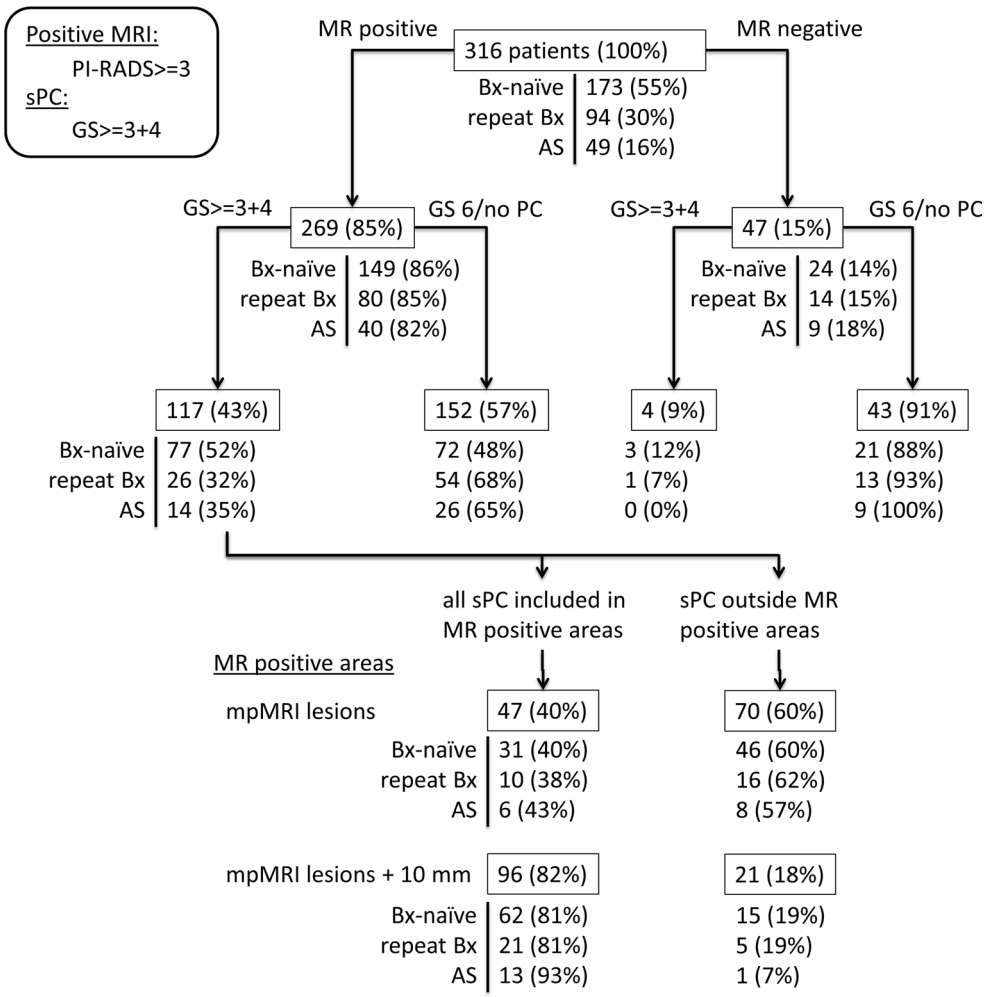

Fig. 2 Distribution of MR imaging results and results of histopathology stratified to the MR findings (MR positive versus MR negative) based on a per-patient basis

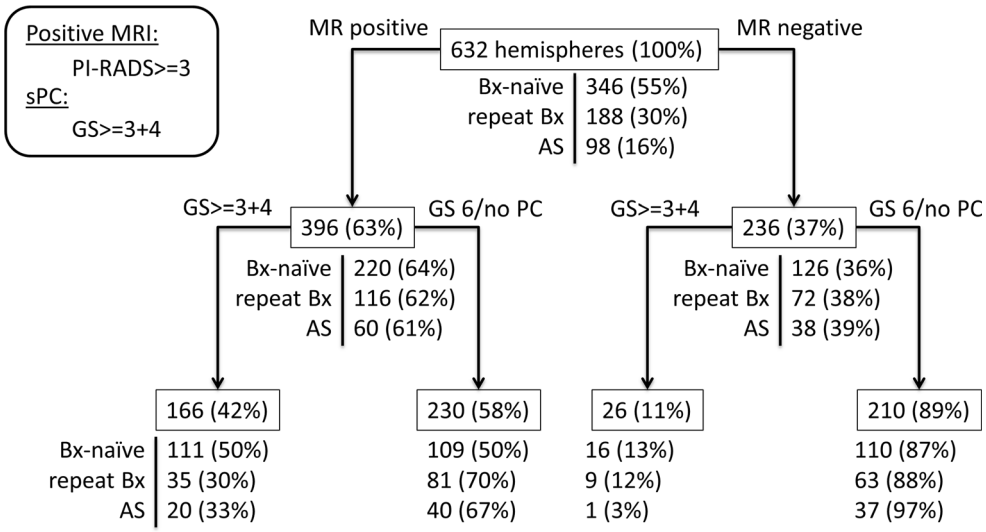

Fig. 3 Distribution of MR imaging results and results of histopathology stratified to the MR findings (MR positive versus MR negative) based on a hemispheric basis

were MR positive and 621 (33%) were MRI negative. Three hundred thirty-seven (26%) out of the 1275 MR-positive sextants harbored sPC, while 938 (74%) were false positive. For MRI-negative sextants, 579 (93%) of 621 were correctly called negative on MRI, while MRI did not detect sPC presence in 42 (7%) of sextants. Sensitivity was 0.73, specificity 0.38, PPV 0.26, and NPV 0.93 (Table 2). Sextant results for sPC definition as ISUP grade ≥ 3 and MRI suspicion defined as PI-RADS ≥ 4 are given in Supplementary Figure 9–11.

Lastly, even though at least one suspicious MRI lesion harboring sPC was identified in 117/121 (97%) patients, there was additional sPC found outside MRI lesions assessed as suspicious (PI-RADS ≥ 3) in 70 men (60%) (Fig. 2). This number was reduced to 21 men (18%) with the added security margin of 10 mm.

Example cases in which sPC remained outside the mpMRI-mapped disease territories despite the use of the security margin are shown in Supplementary Figure 1, while Supplementary Figure 2 shows a case with successful mapping of all sPC (see figure legends for details).

Discussion

The potential of mpMRI to detect sPC is influenced by several issues. First, correct lesion detection by mpMRI occurred in 97% of patients and was comparable to recent publications, using both, combined FTB and SB cores, or radical prostatectomy specimen as reference tests [1, 12, 22]. Hence, on a patient basis, the results generated in clinical routine at our center with dedicated prostate MR readers are in line with the accuracy of a recently published study by Panebianco et al [1]. Missed sPC lesions included only Gleason Score 3 + 4 disease, respectively, ISUP grade 2 lesions. When only PI-RADS ≥ 4 lesions would be considered suspicious, significant cancer would be missed in 18 men (15%). These men had ISUP grade 2 disease in 16/18 cases (89%). Only two cases harbored Gleason score 4 + 3, respectively, ISUP grade 3. Based on these results, three conclusions could be drawn. First, on a patient basis, mpMRI is a sensitive diagnostic tool to detect sPC, missing sPC in 3%. Compared to the reference test of combined targeted and systematic biopsy, the results are in line with recently published data from Ahmed et al and Mortezavi et al, but slightly increased compared to Panebianco et al and De Visschere et al [1, 7, 23, 24]. The NPV is comparable to a recent meta-analysis of Moldovan et al (88%) [10]. Second, these data emphasize the current status of PI-RADS 3 lesions. Although called indeterminate, PI-RADS 3 lesions harbored sPC in 19%. This is in line with the results of the multicentric PRECISION data (12%), the publication of Venderink et al (17%), and the results of Meng et al, using an institutional Likert scale, but increased compared to the data of Ullrich et al (4%) [8, 25–27]. However, based on our results and in line with the PRECISION data and in particular to Venderink et al, an mpMRI Likert score 3–5 should be called cancer suspicious and undergo targeted prostate biopsy [8, 27]. The observed specificity and PPV observed in this study were lower compared to the same definition of csPC in the recently published PROMIS study (0.45 and 0.65). However, sensitivity and NPV are higher compared to PROMIS (0.88 and 0.76). In fact, the performance in this study at a PI-RADS cut-off of ≥ 4 is closer to the PROMIS performance. This might be caused by differences in the sPC prevalence and differences in MR interpretation, as the MRI interpretation in the PROMIS trial was done by an internal University College of London Hospital score, which is quite comparable to PI-RADS but slightly different. While our data at the more sensitive PI-RADS ≥ 3 cut-off are therefore well-suited to examine the distribution of MR-invisible sPC and confirm the ability of MRI to successfully guide biopsies to detect sPC with very high

Table 2 Performance of mpMRI for different PI-RADS cut-offs and different definitions of sPC on a patient basis, for hemispheres, and on a sextant level

Topology	PI-RADS	Gleason/ISUP	Sensitivity	Specificity	PPV	NPV
Patient	≥ 3	≥ 3 + 4 / 2	0.97 (117/121)	0.22 (43/195)	0.43 (117/269)	0.91 (43/47)
		Biopsy-naïve	0.96 (77/80)	0.23 (21/93)	0.52 (77/149)	0.88 (21/24)
		Repeat biopsy	0.96 (26/27)	0.19 (13/67)	0.32 (26/80)	0.93 (13/14)
		AS	1.00 (14/14)	0.26 (9/35)	0.35 (14/40)	1.00 (9/9)
Patient	≥ 3	≥ 4 + 3 / 3	1.00 (41/41)	0.17 (47/275)	0.15 (41/269)	1.00 (47/47)
		Biopsy-naïve	1.00 (32/32)	0.17 (24/141)	0.21 (32/149)	1.00 (24/24)
		Repeat biopsy	1.00 (7/7)	0.16 (14/87)	0.09 (7/80)	1.00 (14/14)
		AS	1.00 (2/2)	0.19 (9/47)	0.05 (2/40)	1.00 (9/9)
Patient	≥ 4	≥ 3 + 4 / 2	0.85 (103/121)	0.52 (102/195)	0.53 (103/196)	0.85 (102/120)
		Biopsy-naïve	0.86 (69/80)	0.55 (51/93)	0.62 (69/111)	0.82 (51/62)
		Repeat biopsy	0.85 (23/27)	0.49 (33/67)	0.40 (23/57)	0.89 (33/37)
		AS	0.79 (11/14)	0.51 (18/35)	0.39 (11/28)	0.86 (18/21)
Patient	≥ 4	≥ 4 + 3 / 3	0.95 (39/41)	0.43 (118/275)	0.20 (39/196)	0.98 (118/120)
		Biopsy-naïve	0.97 (31/32)	0.43 (61/141)	0.28 (31/111)	0.98 (61/62)
		Repeat biopsy	1.00 (7/7)	0.43 (37/87)	0.12 (7/57)	1.00 (37/37)
		AS	0.50 (1/2)	0.43 (20/47)	0.04 (1/28)	0.95 (20/21)
Hemisphere	≥ 3	≥ 3 + 4 / 2	0.86 (166/192)	0.48 (210/440)	0.42 (166/396)	0.89 (210/236)
		Biopsy-naïve	0.87 (111/127)	0.50 (110/219)	0.50 (111/220)	0.87 (110/126)
		Repeat biopsy	0.80 (35/44)	0.44 (63/144)	0.30 (35/116)	0.88 (63/72)
		AS	0.95 (20/21)	0.48 (37/77)	0.33 (20/60)	0.97 (37/38)
Hemisphere	≥ 3	≥ 4 + 3 / 3	0.94 (61/65)	0.41 (232/567)	0.15 (61/396)	0.98 (232/236)
		Biopsy-naïve	0.92 (48/52)	0.41 (122/294)	0.22 (48/220)	0.97 (122/126)
		Repeat biopsy	1.00 (11/11)	0.41 (72/177)	0.09 (11/116)	1.00 (72/72)
		AS	1.00 (2/2)	0.40 (38/96)	0.03 (2/60)	1.00 (38/38)
Hemisphere	≥ 4	≥ 3 + 4 / 2	0.74 (143/192)	0.70 (310/440)	0.52 (143/273)	0.86 (310/359)
		Biopsy-naïve	0.76 (97/127)	0.73 (159/219)	0.62 (97/157)	0.84 (159/189)
		Repeat biopsy	0.68 (30/44)	0.69 (100/144)	0.41 (30/74)	0.88 (100/114)
		AS	0.76 (16/21)	0.66 (51/77)	0.38 (16/42)	0.91 (51/56)
Hemisphere	≥ 4	≥ 4 + 3 / 3	0.85 (55/65)	0.62 (349/567)	0.20 (55/273)	0.97 (349/359)
		Biopsy-naïve	0.85 (44/52)	0.62 (181/294)	0.28 (44/157)	0.96 (181/189)
		Repeat biopsy	0.91 (10/11)	0.64 (113/177)	0.14 (10/74)	0.99 (113/114)
		AS	0.50 (1/2)	0.57 (55/96)	0.02 (1/42)	0.98 (55/56)
Sextant	≥ 3	≥ 3 + 4 / 2	0.67 (254/379)	0.73 (1111/1517)	0.38 (254/660)	0.90 (1111/1236)
		Biopsy-naïve	0.69 (178/259)	0.75 (584/779)	0.48 (178/373)	0.88 (584/665)
		Repeat biopsy	0.61 (52/85)	0.69 (332/479)	0.26 (52/199)	0.91 (332/365)
		AS	0.69 (24/35)	0.75 (195/259)	0.27 (24/88)	0.95 (195/206)
Sextant	≥ 3	≥ 4 + 3 / 3	0.77 (102/133)	0.68 (1205/1763)	0.15 (102/660)	0.97 (1205/1236)
		Biopsy-naïve	0.75 (79/105)	0.68 (639/933)	0.21 (79/373)	0.96 (639/665)
		Repeat biopsy	0.79 (19/24)	0.67 (360/540)	0.10 (19/199)	0.99 (360/365)
		AS	1.00 (4/4)	0.71 (206/290)	0.05 (4/88)	1.00 (206/206)
Sextant	≥ 4	≥ 3 + 4 / 2	0.58 (221/379)	0.86 (1300/1517)	0.50 (221/438)	0.89 (1300/1458)
		Biopsy-naïve	0.62 (160/259)	0.87 (679/779)	0.62 (160/260)	0.87 (679/778)
		Repeat biopsy	0.49 (42/85)	0.84 (402/479)	0.35 (42/119)	0.90 (402/445)
		AS	0.54 (19/35)	0.85 (219/259)	0.32 (19/59)	0.93 (219/235)
Sextant	≥ 4	≥ 4 + 3 / 3	0.68 (91/133)	0.80 (1416/1763)	0.21 (91/438)	0.97 (1416/1458)
		Biopsy-naïve	0.68 (71/105)	0.80 (744/933)	0.27 (71/260)	0.96 (744/778)
		Repeat biopsy	0.71 (17/24)	0.81 (438/540)	0.14 (17/119)	0.98 (438/445)
		AS	0.75 (3/4)	0.81 (234/290)	0.05 (3/59)	1.00 (234/235)

Table 2 (continued)

Topology	PI-RADS	Gleason/ISUP	Sensitivity	Specificity	PPV	NPV
Sextant with a 10-mm margin	≥ 3	≥ 3 + 4 / 2	0.89 (337/379)	0.38 (579/1517)	0.26 (337/1275)	0.93 (579/621)
		Biopsy-naïve	0.89 (230/259)	0.38 (296/779)	0.32 (230/713)	0.91 (296/325)
		Repeat biopsy	0.87 (74/85)	0.37 (179/479)	0.20 (74/374)	0.94 (179/190)
		AS	0.94 (33/35)	0.40 (104/259)	0.18 (33/188)	0.98 (104/106)
Sextant with a 10-mm margin	≥ 3	≥ 4 + 3 / 3	0.95 (126/133)	0.35 (614/1763)	0.10 (126/1275)	0.99 (614/621)
		Biopsy-naïve	0.93 (98/105)	0.34 (318/933)	0.14 (98/713)	0.98 (318/325)
		Repeat biopsy	1.00 (24/24)	0.35 (190/540)	0.06 (24/374)	1.00 (190/190)
		AS	1.00 (4/4)	0.37 (106/290)	0.02 (4/188)	1.00 (106/106)
Sextant with a 10-mm margin	≥ 4	≥ 3 + 4 / 2	0.79 (300/379)	0.61 (923/1517)	0.34 (300/894)	0.92 (923/1002)
		Biopsy-naïve	0.81 (210/259)	0.60 (471/779)	0.41 (210/518)	0.91 (471/520)
		Repeat biopsy	0.73 (62/85)	0.62 (296/479)	0.25 (62/245)	0.93 (296/319)
		AS	0.80 (28/35)	0.60 (156/259)	0.21 (28/131)	0.96 (156/163)
Sextant with a 10-mm margin	≥ 4	≥ 4 + 3 / 3	0.88 (117/133)	0.56 (986/1763)	0.13 (117/894)	0.98 (986/1002)
		Biopsy-naïve	0.89 (93/105)	0.54 (508/933)	0.18 (93/518)	0.98 (508/520)
		Repeat biopsy	0.88 (21/24)	0.59 (316/540)	0.09 (21/245)	0.99 (316/319)
		AS	0.75 (3/4)	0.56 (162/290)	0.02 (3/131)	0.99 (162/163)

PI-RADS Prostate Imaging Reporting and Data System, *PPV* positive predictive value, *NPV* negative predictive value, *AS* active surveillance

sensitivity, in combination with the main result of this study of some significant disease being invisible to MRI they indicate that the exclusion of sPC and therewith the avoidance of biopsies by MRI is more variable and requires further multi-institutional assessment and improvement of MR technique and interpretation. In addition, the gain in sensitivity resulting from calling PI-RADS 3–5 lesions suspicious comes at the risk of decreasing the specificity. This is mainly driven by calling PI-RADS 3 lesions cancer suspicious. In our cohort, 19% of PI-RADS 3 lesions harbored csPC, leading to a high number of false-positive lesions in this category. However, this is in line with the results of the recently published PRECISION trial (12% detection of csPC) [8] and the publication by Meng et al [26], but higher compared to Ullrich et al (4%) [25]. The specificity in our cohort might also be affected by differences in interpreting PI-RADS between readers and institutions, as mentioned in 25% of the MRI scans performed in the PRECISION trial, that have been picked for expert reading [8].

With the development of focal therapy options for PC treatment, there is a need for accurate determination of the eligibility and spatial treatment planning for such procedures. Kenigsberg et al reported that GP 4 extra-focal disease defined as any GP 4 not detected by mpMRI and TRUS systematic biopsy outside of an ablation zone was present in 15/59 (25%) of cases [9]. For focal treatment options, analysis of the accuracy of mpMRI on sextant or hemisphere basis is mandatory. In addition, the reference test for MRI accuracy is important. Our study provides an assessment of the performance of mpMRI without biopsy compared to extended biopsy mapping. It is expected that the larger number of SB in this study provides a better assessment of true histopathology and can account for most of the disease found in RP specimen, as demonstrated previously [12]. The 18% of sPC outside the mpMRI targets plus a 10-mm security margin compares well with the 25% as there probably remains a small number of undiagnosed sPC by our biopsy approach [9]. Based on hemispheric analysis, mpMRI correctly ruled out sPC in 89% of hemispheres. This is important for hemigland treatment, e.g., in high-intensity focused ultrasound. Interestingly, a 10-mm safety margin around the MRI lesion to attenuate wide-known significant underestimation of the tumor lesion volume on MRI, as propagated by Le Nobin et al, did not influence the detection accuracy on hemispheric basis (not shown in the results) [19, 28, 29]. Thus, our results do not support that mpMRI and targeted biopsies alone could be safely used as an upfront approach prior to focal treatment. As a consequence, a systematic biopsy approach is still necessary to determine near-total whole-gland pathology for a secure hemigland treatment.

On sextant analysis, the results (67% sensitivity, 90% NPV) were comparable with a previous analysis using whole-gland specimen as reference test [12] and also comparable to a meta-analysis of Moldovan et al [10]. In our study, the NPV of 90% is achieved by considering PI-RADS 3–5 lesions as cancer suspicious, while in the previous study, PI-RADS 2 lesions have been called suspicious to gain maximum patient security, including potential over detection [12]. This difference likely represents a performance gain since the introduction of PI-RADS version 2. In conclusion, only applying targeted cores to PI-RADS 3–5 lesions seems to be appropriate with a satisfying NPV. Interestingly, when applying a 10-mm safety margin, the rate of missing sPC decreased to 7%, supporting saturation biopsy of the target lesion, as proposed by Le Nobin et al [19]. In addition, to gain maximum security, systematic biopsies

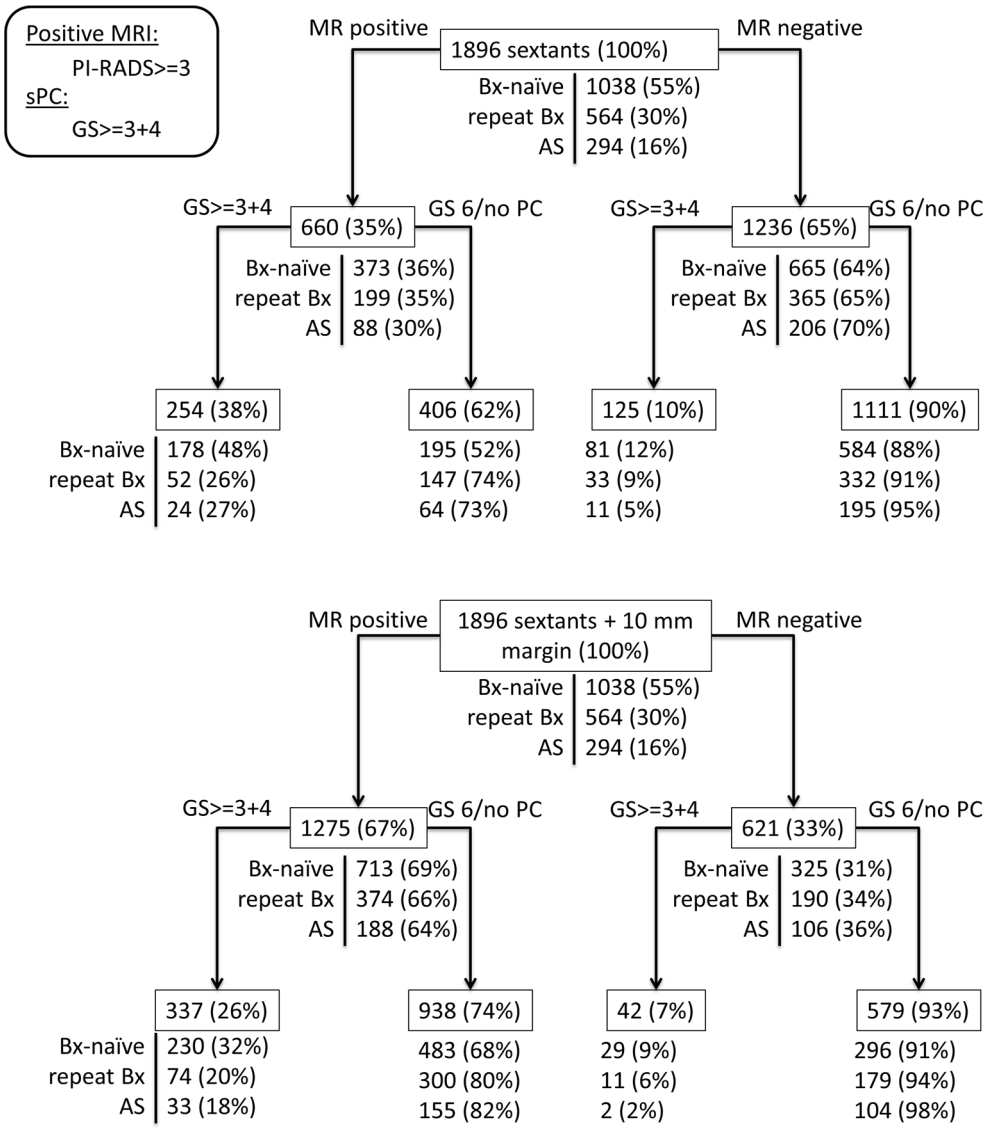

Fig. 4 Distribution of MR imaging results and results of histopathology stratified to the MR findings (MR positive versus MR negative) based on sextant level

still cannot be omitted, supporting the recent European Association of Urology (EAU) guidelines recommendation [5].

Our study is subject to several limitations. We did not have radical prostatectomy (RP) data available, which serve as reference histopathological assessment. However, the sensitivity of the extended systematic and targeted biopsy performed here has been shown to detect 97% of sPC compared to RP specimen [12] and confirmed it as a robust reference test compared to the known limited performance of the 12-core TRUS as a screening test as recently confirmed by the PROMIS and PRECISION trials [7, 8]. The study design was retrospective; however, all eligible patients undergoing MRI and fusion biopsy were analyzed. MRI interpretation at a high-volume center might represent a potential bias and limit the generalizability of our analysis. This being said, to achieve high-confidence MRI results, special training, accreditation, and certification of radiologists with special interest in prostate MR reporting is mandatory. In this context, one should be aware of potential differences across MR reading [30]. Lastly, the definition of the sextant scheme according to the Ginsburg study is not the only systematic option. Alternatively, one could employ the 27-region scheme published by Dickinson et al, which was used for concordance analyses previously [12, 31–33].

Conclusion

MpMRI mapping agreed well with histopathology, with an overall excellent sensitivity for sPC and, at the sPC prevalence observed in the study cohort, very good negative predictive value to rule out sPC on a patient basis. However, 18% of sPC was outside the mpMRI-mapped prostate tissue, quantifying known limitations of MRI for assessment of disease extent. While complete spatial mapping of sPC by mpMRI appears limited, detection of the presence of sPC is possible at very high sensitivity based on the presence of an MR index lesion.

Funding The authors state that this work has not received any funding.

Compliance with ethical standards

Guarantor The scientific guarantor of this publication is Heinz-Peter Schlemmer.

Conflict of interest David Bonekamp is a speaker for Profound Medical Inc.

Patrick Schelb has nothing to declare.

Manuel Wiesenfarth has nothing to declare.

Tristan Anselm Kuder has nothing to declare.

Fenja Deister has nothing to declare.

Albrecht Stenzinger declares the following: consulting fee and payment for lectures: Astra Zeneca, BMS, Novartis, Roche, Illumina, Thermo Fisher; travel support: Astra Zeneca, BMS, Novartis, Illumina, Thermo Fisher; board member: Astra Zeneca, BMS, Novartis, Thermo Fisher.

Joanne Nyarangi-Dix has nothing to declare.

Matthias Röthke declares consulting fee and payment for lectures: Siemens Healthineers, Curagita AG.

Markus Hohenfellner has nothing to declare.

Heinz-Peter Schlemmer declares the following: consulting fee or honorarium: Siemens, Curagita, Profound, Bayer; travel support: Siemens, Curagita, Profound, Bayer; board member: Curagita; consultancy: Curagita, Bayer; grants/grants pending: BMBF, Deutsche Krebshilfe, Dietmar-Hopp-Stiftung, Roland-Ernst-Stiftung; payment for lectures: Siemens, Curagita, Profound, Bayer.

Jan Philipp Radtke declares payment for consultant work from Saegeling Medizintechnik and Siemens Heathineers and for development of educational presentations from Saegeling Medizintechnik.

Statistics and biometry Manuel Wiesenfarth is the lead statistician and co-author on this paper.

Informed consent Written informed consent was waived by the Ethics Commission.

Ethical approval Ethical approval was obtained.

Study subjects or cohorts overlap The examined cohort was subject to a recently published study (Bonekamp D, Kohl S, Wiesenfarth M et al (2018) Radiomic machine learning for characterization of prostate lesions by MRI: comparison to ADC values. Radiology 31:173064. https://doi.org/10.1148/radiol.2018173064. Focusing on apparent diffusion coefficient and radiomics for lesion classification; however, sextant-level histopathology to mpMRI mapping has not been previously performed.

Methodology
- retrospective
- diagnostic study
- single-center study

References

1. Panebianco V, Barchetti G, Simone G et al (2018) Negative multiparametric magnetic resonance imaging for prostate cancer : what's next ? Eur Urol. https://doi.org/10.1016/j.eururo.2018.03.007
2. Barentsz JO, Richenberg J, Clements R et al (2012) ESUR prostate MR guidelines 2012. Eur Radiol 22:746–757. https://doi.org/10.1007/s00330-011-2377-y
3. Siddiqui MM, Rais-Bahrami S, Truong H et al (2013) Magnetic resonance imaging/ultrasound-fusion biopsy significantly upgrades prostate cancer versus systematic 12-core transrectal ultrasound biopsy. Eur Urol 64:713–719. https://doi.org/10.1016/j.eururo.2013.05.059
4. Radtke JP, Kuru TH, Boxler S et al (2015) Comparative analysis of transperineal template saturation prostate biopsy versus magnetic resonance imaging targeted biopsy with magnetic resonance imaging-ultrasound fusion guidance. J Urol. https://doi.org/10.1016/j.juro.2014.07.098
5. Mottet N, Bellmunt J, Bolla M et al (2017) EAU-ESTRO-SIOG guidelines on prostate Cancer. Part 1: screening, diagnosis, and local treatment with curative intent. Eur Urol 71:618–629. https://doi.org/10.1016/j.eururo.2016.08.003
6. Kasivisvanathan V, Dufour R, Moore CM et al (2013) Transperineal magnetic resonance image targeted prostate biopsy versus transperineal template prostate biopsy in the detection of clinically significant prostate cancer. J Urol 189:860–866. https://doi.org/10.1016/j.juro.2012.10.009
7. Ahmed HU, El-Shater Bosaily A, Brown LC et al (2017) Diagnostic accuracy of multi-parametric MRI and TRUS biopsy in prostate cancer (PROMIS): a paired validating confirmatory study. Lancet 6736:32401–32401. https://doi.org/10.1016/S0140-6736(16)32401-1
8. Kasivisvanathan V, Rannikko AS, Borghi M et al (2018) MRI-targeted or standard biopsy for prostate-cancer diagnosis. N Engl J Med. https://doi.org/10.1056/NEJMoa1801993
9. Kenigsberg AP, Llukani E, Deng FM, Melamed J, Zhou M, Lepor H (2018) The use of magnetic resonance imaging to predict oncological control among candidates for focal ablation of prostate cancer. Urology 112:121–125. https://doi.org/10.1016/j.urology.2017.10.014
10. Moldovan PC, Van den Broeck T, Sylvester R et al (2017) What is the negative predictive value of multiparametric magnetic resonance imaging in excluding prostate cancer at biopsy ? A systematic review and meta-analysis from the european association of urology prostate cancer guidelines panel. Eur Urol. https://doi.org/10.1016/j.eururo.2017.02.026
11. Borofsky S, George AK, Gaur S et al (2018) What are we missing ? False-negative cancers at multiparametric MR imaging of the prostate 1. Radiology 0:1–10. https://doi.org/10.1148/radiol.2017152877
12. Radtke JP, Schwab C, Wolf MB et al (2016) Multiparametric magnetic resonance imaging (MRI) and MRI – transrectal ultrasound fusion biopsy for index tumor detection : correlation with radical prostatectomy specimen. Eur Urol 70:846–853. https://doi.org/10.1016/j.eururo.2015.12.052
13. Bonekamp D, Kohl S, Wiesenfarth M et al (2018) Radiomic machine learning for characterization of prostate lesions by MRI: comparison to ADC values. Radiology. https://doi.org/10.1148/radiol.2018173064
14. Moore CM, Kasivisvanathan V, Eggener S et al (2013) Standards of reporting for MRI-targeted biopsy studies (START) of the prostate: recommendations from an International Working Group. Eur Urol 64:544–552. https://doi.org/10.1016/j.eururo.2013.03.030
15. Weinreb JC, Barentsz JO, Choyke PL et al (2015) PI-RADS prostate imaging - reporting and data system: 2015, version 2. Eur Urol 69(1):16–40. https://doi.org/10.1016/j.eururo.2015.08.052
16. Kuru TH, Wadhwa K, Chang RT et al (2013) Definitions of terms, processes and a minimum dataset for transperineal prostate biopsies: a standardization approach of the Ginsburg Study Group for Enhanced Prostate Diagnostics. BJU Int 112:568–577. https://doi.org/10.1111/bju.12132
17. Nolden M, Zelzer S, Seitel A et al (2013) The medical imaging interaction toolkit: challenges and advances: 10 years of open-

source development. Int J Comput Assist Radiol Surg 8:607–620. https://doi.org/10.1007/s11548-013-0840-8
18. Fritzsche KH, Neher PF, Reicht I et al (2012) MITK diffusion imaging. Methods Inf Med 51:441–448. https://doi.org/10.3414/ME11-02-0031
19. Le Nobin J, Rosenkrantz AB, Villers A et al (2015) Image guided focal therapy of MRI-visible prostate cancer: defining a 3D treatment margin based on MRI-histology co-registration analysis. J Urol 1–7. https://doi.org/10.1016/j.juro.2015.02.080
20. R Development Core Team R (2015) R: a language and environment for statistical computing. Foundation for Statistical Computing, Vienna, Austria. http://www.R-project.org/. Accessed 12 Aug 2018
21. Bossuyt PM, Reitsma JB, Bruns DE et al (2003) Towards complete and, accurate reporting of studies of diagnostic accuracy: the STARD initiative. Radiology 226:24–28. https://doi.org/10.1136/bmj.326.7379.41
22. Baco E, Ukimura O, Rud E et al (2015) Magnetic resonance imaging – transectal ultrasound image-fusion biopsies accurately characterize the index tumor: correlation with step-sectioned radical prostatectomy specimens in 135 patients. Eur Urol 67:787–794. https://doi.org/10.1016/j.eururo.2014.08.077
23. Mortezavi A, Märzendorfer O, Donati OF et al (2018) Diagnostic accuracy of mpMRI and fusion-guided targeted biopsy evaluated by transperineal template saturation prostate biopsy for the detection and characterization of prostate cancer. J Urol. https://doi.org/10.1016/j.juro.2018.02.067
24. De Visschere PJ, Naesens L, Libbrecht L et al (2016) What kind of prostate cancers do we miss on multiparametric magnetic resonance imaging? Eur Radiol 26:1098–1107. https://doi.org/10.1007/s00330-015-3894-x
25. Ullrich T, Quentin M, Arsov C et al (2017) Risk stratification of "equivocal" PI-RADS lesions in mp-MRI of the prostate. J Urol. https://doi.org/10.1016/j.juro.2017.09.074
26. Meng X, Rosenkrantz AB, Mendhiratta N et al (2016) Relationship of pre-biopsy multiparametric MRI and biopsy indication with MRI-US fusion-targeted prostate biopsy outcomes. Eur Urol 69:512–517. https://doi.org/10.1016/j.eururo.2015.06.005
27. Venderink W, Van Luijtelaar A, Bomers JG et al (2017) Results of targeted biopsy in men with magnetic resonance imaging lesions classified equivocal , likely or highly Likely to be clinically significant prostate cancer. Eur Urol 1–8. https://doi.org/10.1016/j.eururo.2017.02.021
28. Le Nobin J, Orczyk C, Deng FM et al (2014) Prostate tumour volumes: evaluation of the agreement between magnetic resonance imaging and histology using novel co-registration software. BJU Int 114:E105–E112. https://doi.org/10.1111/bju.12750
29. Bratan F, Melodelima C, Souchon R et al (2015) How accurate is multiparametric MR imaging in evaluation of prostate cancer volume? Radiology 275:144–154. https://doi.org/10.1148/radiol.14140524
30. Sonn GA, Fan RE, Ghanouni P et al (2017) Prostate magnetic resonance imaging interpretation varies substantially across radiologists. Eur Urol Focus. https://doi.org/10.1016/j.euf.2017.11.010
31. Turkbey B, Pinto PA, Mani H et al (2010) Prostate cancer: value of multiparametric MR imaging at 3 T for detection–histopathologic correlation. Radiology 255:89–99. https://doi.org/10.1148/radiol.09090475
32. Rosenkrantz AB, Deng FM, Kim S et al (2012) Prostate cancer: multiparametric mri for index lesion localization - a multiple-reader study. AJR Am J Roentgenol 199:830–837. https://doi.org/10.2214/AJR.11.8446
33. Dickinson L, Ahmed HU, Allen C et al (2011) Magnetic resonance imaging for the detection, localisation, and characterisation of prostate cancer: recommendations from a European consensus meeting. Eur Urol 59:477–494. https://doi.org/10.1016/j.eururo.2010.12.009